Effects of local features of the inflaton potential on the spectrum and bispectrum of primordial curvature perturbations

Alexander Gallego Cadavid
University of Antioquia

Partially based on: Eur. Phys. J. **C75**, 589 (2015) and Eur. Phys. J. **C76**, 385 (2016)
Co-Authors: Antonio Enea Romano, University of Antioquia and Stefano Gariazzo, University of Torino

September 30, 2016

Motivation

Motivation

Inflation

- Accounts for the observation of anisotropies in the CMB and formation of large scale structures.

Motivation

Inflation

- Accounts for the observation of anisotropies in the CMB and formation of large scale structures.

Features in the potential

- Suppression of the power spectrum of the CMB at large scales, $l < 30$.
- Theoretical and observational evidence of a dip in the power spectrum of the CMB around $l \simeq 20$.

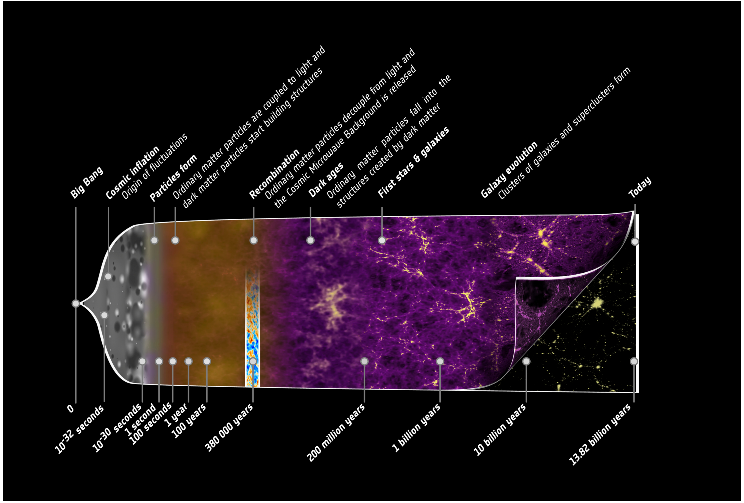

Figure: Evolution of the universe. Image credit: ESA

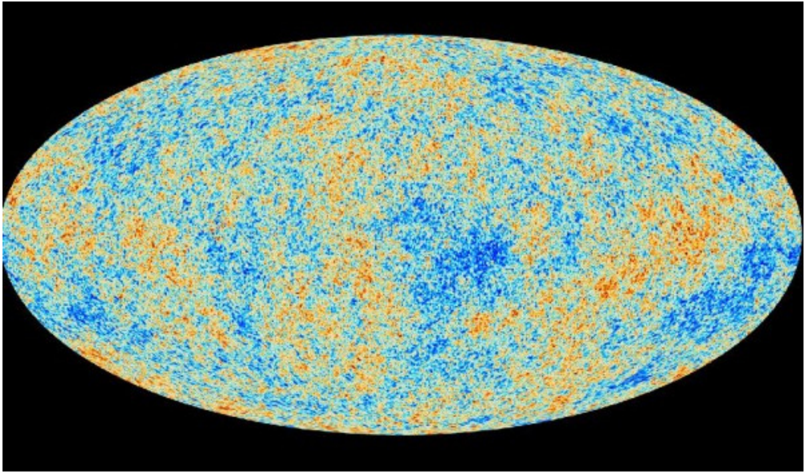

Figure: All-sky image of the CMB by Planck. Hotter (colder) regions of the sky are represented by red (blue). Image credit: ESA and the Planck Collaboration 2013.

Temperature anisotropies

$$\frac{T_0 - T}{T_0}(\hat{n}) \equiv \Theta(t_0, \vec{x}, -\hat{n}) = \sum_{l,m} a_{lm} Y_{lm}(\hat{n}). \tag{1}$$

The transfer function

For an arbitrary perturbation A at time t

$$A(t, \vec{k}) = A(t, k)\zeta(t_i, \vec{k}), \tag{2}$$

where A is the transfer function.

The transfer function

For an arbitrary perturbation A at time t

$$A(t, \vec{k}) = \mathcal{A}(t, k)\zeta(t_i, \vec{k}), \tag{2}$$

where $\mathcal{A}$ is the transfer function.

Then the two-point function is

$$\left\langle A(t, \vec{k})A(t, \vec{k}') \right\rangle = \mathcal{A}(t, k)^2 P_\zeta(k)\delta^{(3)}(\vec{k} - \vec{k}'). \tag{3}$$

Spectrum of temperature anisotropies

$$\langle a_{lm} a^*_{l'm'} \rangle = \delta_{ll'} \delta_{mm'} \left[\frac{1}{2\pi^2} \int \frac{dk}{k} \Theta(t_0, k)^2 P_\zeta(k) \right] = \delta_{ll'} \delta_{mm'} C_l = \frac{2\pi \delta_{ll'} \delta_{mm'}}{l(l+1)} D_l \,, \tag{4}$$

$\Theta(t_0, k)$ is the transfer function for the photon multipoles.

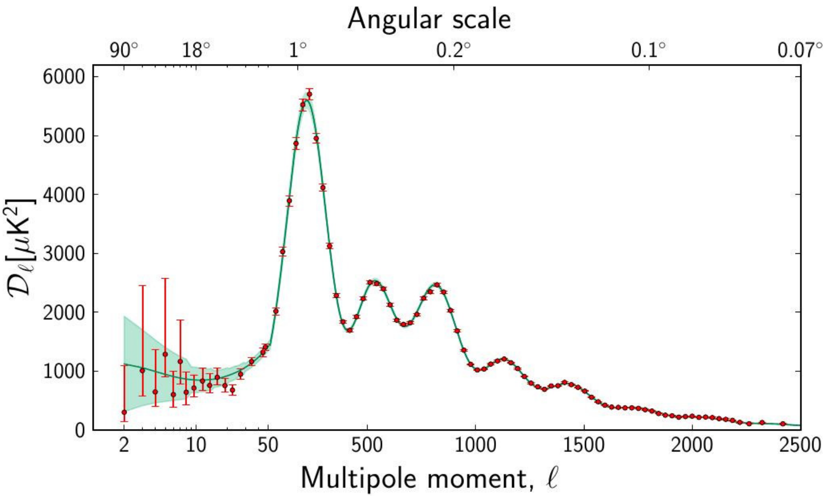

Figure: The power spectrum of the CMB. The green line is the prediction from the ΛCDM model. Image credit: Planck.

$$S = \int d^4x \sqrt{-g} \left[\frac{1}{2} M_{Pl}^2 R - \frac{1}{2} g^{\mu\nu} \partial_\mu \phi \partial_\nu \phi - V(\phi) \right] . \tag{5}$$

$$S = \int d^4x\sqrt{-g}\left[\frac{1}{2}M_{Pl}^2 R - \frac{1}{2}g^{\mu\nu}\partial_\mu\phi\partial_\nu\phi - V(\phi)\right] . \tag{5}$$

The background equations are

$$H^2 \equiv \left(\frac{\dot{a}}{a}\right)^2 = \frac{1}{3M_{Pl}^2}\left(\frac{1}{2}\dot{\phi}^2 + V(\phi)\right), \tag{6}$$

$$\ddot{\phi} + 3H\dot{\phi} + \partial_\phi V = 0. \tag{7}$$

$$S = \int d^4x\sqrt{-g}\left[\frac{1}{2}M_{Pl}^2 R - \frac{1}{2}g^{\mu\nu}\partial_\mu\phi\partial_\nu\phi - V(\phi)\right] . \tag{5}$$

The background equations are

$$H^2 \equiv \left(\frac{\dot{a}}{a}\right)^2 = \frac{1}{3M_{Pl}^2}\left(\frac{1}{2}\dot{\phi}^2 + V(\phi)\right), \tag{6}$$

$$\ddot{\phi} + 3H\dot{\phi} + \partial_\phi V = 0. \tag{7}$$

The slow-roll parameters

$$\epsilon \equiv -\frac{\dot{H}}{H^2} \quad , \quad \eta \equiv \frac{\dot{\epsilon}}{\epsilon H} . \tag{8}$$

We consider the local feature potential

$$V(\phi) = V_0 + \lambda e^{-\left(\frac{\phi-\phi_0}{\sigma}\right)^2} \tag{9}$$

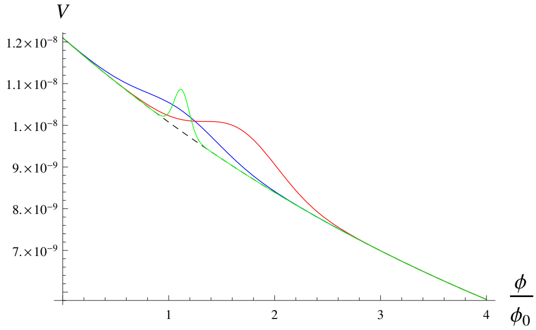

Figure: The feature potential with Power Law Inflation $V_0 = Ae^{-\sqrt{\frac{2}{q}}\frac{\phi}{M_{Pl}}}$. Gallego et al. Eur. Phys. J. **C76**, 385 (2016).

Local features (LF) Vs Branch features (BF)

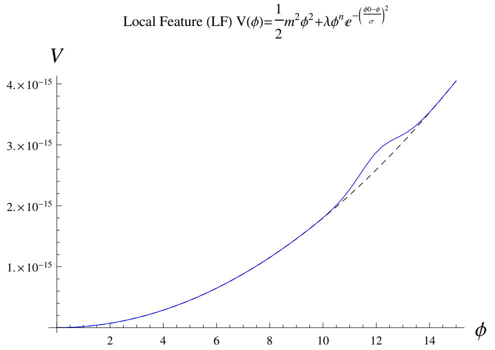

Figure: Local features $V(\phi) = V_0 + \lambda e^{-(\frac{\phi-\phi_0}{\sigma})^2}$.

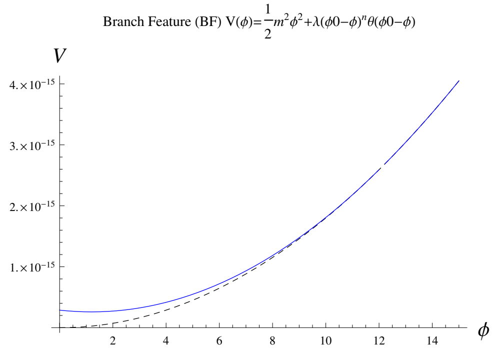

Branch features $V(\phi) = V_0 + \lambda(\phi_0 - \phi)^n \theta(\phi_0 - \phi)$.

We perform the perturbations

$$\phi(t,\vec{x}) = \bar{\phi}(t) + \delta\phi(t,\vec{x}), \tag{10}$$

$$g_{\mu\nu}(t,\vec{x}) = \bar{g}_{\mu\nu}(t) + \delta g_{\mu\nu}(t,\vec{x}). \tag{11}$$

The ADM formalism

$$\begin{aligned} ds^2 &= N^2\,dt^2 - h_{ij}\left(N^i\,dt + dx^i\right)\left(N^j\,dt + dx^j\right), \\ &= \left(N^2 - N_i N^i\right) dt^2 - 2N_i\,dtdx^i - h_{ij}\,dx^i dx^j, \end{aligned} \tag{12}$$

where $N(t, \vec{x})$ is called the *lapse function* while $N^i(t, \vec{x})$ is the *shift vector*.

The action

$$S = \frac{1}{2}\int d^4x\sqrt{h}\left\{N\mathcal{R}^{(3)} + \frac{1}{N}(E_{ij}E^{ij} - E^2) + \frac{1}{N}(\dot{\phi} - N^i\partial_i\phi)^2 - Nh^{ij}\partial_i\phi\partial_j\phi - 2NV(\phi)\right\}. \quad (13)$$

The action

$$S = \frac{1}{2}\int d^4x\sqrt{h}\left\{N\mathcal{R}^{(3)} + \frac{1}{N}(E_{ij}E^{ij} - E^2) + \frac{1}{N}(\dot{\phi} - N^i\partial_i\phi)^2 - Nh^{ij}\partial_i\phi\partial_j\phi - 2NV(\phi)\right\}. \tag{13}$$

General parametrisation of the metric

$$N = 1 + 2\Phi(t,\vec{x}),\ \ N^i = \partial^i B(t,\vec{x}),\ \ h_{ij} = a^2\left[(1+2\zeta(t,\vec{x}))\,\delta_{ij} + \partial_i\partial_j\xi(t,\vec{x})\right]. \tag{14}$$

The action

$$S = \frac{1}{2}\int d^4x\sqrt{h}\left\{N\mathcal{R}^{(3)} + \frac{1}{N}(E_{ij}E^{ij} - E^2) + \frac{1}{N}(\dot{\phi} - N^i\partial_i\phi)^2 - Nh^{ij}\partial_i\phi\partial_j\phi - 2NV(\phi)\right\}. \tag{13}$$

General parametrisation of the metric

$$N = 1 + 2\Phi(t,\vec{x}),\ \ N^i = \partial^i B(t,\vec{x}),\ \ h_{ij} = a^2\left[(1 + 2\zeta(t,\vec{x}))\,\delta_{ij} + \partial_i\partial_j\xi(t,\vec{x})\right]. \tag{14}$$

General parametrisation of the field

$$\phi = \phi_0(t) + \delta\phi(t,\vec{x}). \tag{15}$$

Comoving gauge ζ

Varying with respect to N and N^i yields

$$\begin{aligned} \mathcal{R}^{(3)} - N^{-2}(E_{ij}E^{ij} - E^2) - N^{-2}(\dot{\phi} - N^i\partial_i\phi)^2 - h^{ij}\partial_i\phi\partial_j\phi - 2V = 0\,, \\ \hat{\nabla}_j\left[N^{-1}(E_i{}^j - \delta_i{}^j E)\right] - N^{-1}(\dot{\phi} - N^j\partial_j\phi)\partial_i\phi = 0. \end{aligned} \tag{16}$$

Comoving gauge ζ

Varying with respect to N and N^i yields

$$\mathcal{R}^{(3)} - N^{-2}(E_{ij}E^{ij} - E^2) - N^{-2}(\dot{\phi} - N^i\partial_i\phi)^2 - h^{ij}\partial_i\phi\partial_j\phi - 2V = 0\,, \tag{16}$$
$$\hat{\nabla}_j\left[N^{-1}(E_i{}^j - \delta_i{}^j E)\right] - N^{-1}(\dot{\phi} - N^j\partial_j\phi)\partial_i\phi = 0.$$

Redefining the time and spatial coordinates

$$N = 1 + 2\Phi(t,\vec{x}), \quad N^i = \partial^i B(t,\vec{x}), \quad h_{ij} = a^2 e^{2\zeta(t,\vec{x})}\delta_{ij}, \quad \phi = \phi_0(t)\,. \tag{17}$$

Comoving gauge ζ

Varying with respect to N and N^i yields

$$\mathcal{R}^{(3)} - N^{-2}(E_{ij}E^{ij} - E^2) - N^{-2}(\dot{\phi} - N^i\partial_i\phi)^2 - h^{ij}\partial_i\phi\partial_j\phi - 2V = 0\,, \qquad (16)$$
$$\hat{\nabla}_j\left[N^{-1}(E_i{}^j - \delta_i{}^j E)\right] - N^{-1}(\dot{\phi} - N^j\partial_j\phi)\partial_i\phi = 0.$$

Redefining the time and spatial coordinates

$$N = 1 + 2\Phi(t,\vec{x}), \quad N^i = \partial^i B(t,\vec{x}), \quad h_{ij} = a^2 e^{2\zeta(t,\vec{x})}\delta_{ij}, \quad \phi = \phi_0(t)\,. \qquad (17)$$

To first order in the perturbations

$$\Phi = \frac{1}{2}\frac{\dot{\zeta}}{H} \qquad \text{and} \qquad B = -\frac{1}{a^2 H}\zeta + \frac{1}{2}\epsilon\partial^{-2}\dot{\zeta}. \qquad (18)$$

Second order action and the mode equation

$$S_2 = \int dt d^3x \left[a^3 \epsilon \dot{\zeta}^2 - a\epsilon \partial_k \zeta \partial^k \zeta \right] . \quad (19)$$

Second order action and the mode equation

$$S_2 = \int dtd^3x \left[a^3\epsilon\dot{\zeta}^2 - a\epsilon\partial_k\zeta\partial^k\zeta\right]. \tag{19}$$

Quantizing the curvature perturbation in Fourier space

$$\hat{\zeta}(t,\vec{k}) = \zeta_k(t)\hat{a}_{\vec{k}} + \zeta^*_{-k}(t)\hat{a}^\dagger_{-\vec{k}}. \tag{20}$$

Second order action and the mode equation

$$S_2 = \int dtd^3x \left[a^3\epsilon\dot{\zeta}^2 - a\epsilon\partial_k\zeta\partial^k\zeta\right] . \quad (19)$$

Quantizing the curvature perturbation in Fourier space

$$\hat{\zeta}(t,\vec{k}) = \zeta_k(t)\hat{a}_{\vec{k}} + \zeta^*_{-k}(t)\hat{a}^\dagger_{-\vec{k}} . \quad (20)$$

The equation of motion gives

$$\zeta''_k + 2\frac{z'}{z}\zeta'_k + k^2\zeta_k = 0, \quad (21)$$

where $z \equiv a\sqrt{2\epsilon}$ and k is the comoving wave number.

The two-point function of primordial perturbations

$$\left\langle \hat{\zeta}_{\vec{k}_1} \hat{\zeta}_{\vec{k}_2} \right\rangle = (2\pi)^3 \frac{2\pi^2}{k^3} P_\zeta(k) \delta^{(3)}(\vec{k}_1 + \vec{k}_2) \,. \tag{22}$$

The two-point function of primordial perturbations

$$\left\langle \hat{\zeta}_{\vec{k}_1} \hat{\zeta}_{\vec{k}_2} \right\rangle = (2\pi)^3 \frac{2\pi^2}{k^3} P_\zeta(k) \delta^{(3)}(\vec{k}_1 + \vec{k}_2) \,. \tag{22}$$

The power spectrum of curvature perturbations ζ

$$P_\zeta(k) \equiv \frac{2k^3}{(2\pi)^2} |\zeta_k|^2 . \tag{23}$$

Temperature angular power spectrum of the CMB

$$\langle a_{lm} a^*_{l'm'} \rangle = \delta_{ll'} \delta_{mm'} \left[\frac{1}{2\pi^2} \int \frac{dk}{k} \Theta(t_0, k)^2 P_\zeta(k) \right] = \frac{2\pi \delta_{ll'} \delta_{mm'}}{l(l+1)} D_l \,. \tag{24}$$

Third Order Action

$$S_3 = \int dt d^3x \left[-a^3 \epsilon \eta \zeta \dot{\zeta}^2 - \frac{1}{2} a \epsilon \eta \zeta \partial_k \zeta \partial^k \zeta \right] .$$

Third Order Action

$$S_3 = \int dt d^3x \left[-a^3 \epsilon \eta \zeta \dot{\zeta}^2 - \frac{1}{2} a \epsilon \eta \zeta \partial_k \zeta \partial^k \zeta \right] .$$

Bispectrum

$$\left\langle \hat{\zeta}(\vec{k}_1, t) \hat{\zeta}(\vec{k}_2, t) \hat{\zeta}(\vec{k}_3, t) \right\rangle = (2\pi)^3 B_\zeta(k_1, k_2, k_3) \delta^{(3)}(\vec{k}_1 + \vec{k}_2 + \vec{k}_3) .$$

Third Order Action

$$S_3 = \int dtd^3x \left[-a^3 \epsilon \eta \zeta \dot{\zeta}^2 - \frac{1}{2} a \epsilon \eta \zeta \partial_k \zeta \partial^k \zeta \right] .$$

Bispectrum

$$\left\langle \hat{\zeta}(\vec{k}_1, t) \hat{\zeta}(\vec{k}_2, t) \hat{\zeta}(\vec{k}_3, t) \right\rangle = (2\pi)^3 B_\zeta(k_1, k_2, k_3) \delta^{(3)}(\vec{k}_1 + \vec{k}_2 + \vec{k}_3) .$$

F_{NL} Functions

$$F_{NL}(k_1, k_2, k_3) \equiv \frac{10}{3(2\pi)^4} \frac{(k_1 k_2 k_3)^3}{k_1^3 + k_2^3 + k_3^3} \frac{B_\zeta(k_1, k_2, k_3)}{P_\zeta^2} .$$

Primordial spectrum of curvature perturbations

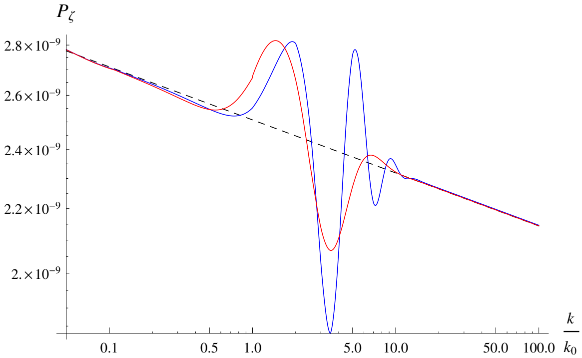

Figure: The P_ζ is plotted for different values of λ, ϕ, and σ. The dashed black lines correspond to the featureless behavior. $V(\phi) = V_0 + \lambda e^{-(\frac{\phi-\phi_0}{\sigma})^2}$. A. Gallego et al. Eur. Phys. J. **C76**, 385 (2016).

Difference between branch and local features

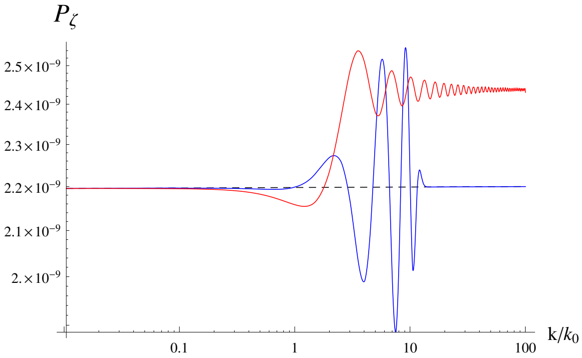

Figure: P_ζ for LF $V(\phi) = V_0(\phi) + \lambda e^{-(\frac{\phi-\phi_0}{\sigma})^2}$ (blue) and BF $V(\phi) = V_0(\phi) + \lambda\theta(\phi_0 - \phi)$ (red), where $V_0(\phi) = V_{vac} + \frac{1}{2}m^2\phi^2$. A. Gallego et al. Eur. Phys. J. **C75**, 589 (2015).

Difference between branch and local features

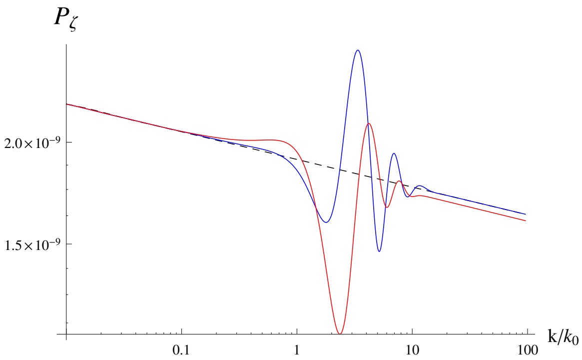

Figure: P_ζ for LF $V(\phi) = V_0(\phi) + \lambda e^{-(\frac{\phi-\phi_0}{\sigma})^2}$ (blue) and BF $V(\phi) = V_0(\phi) + \frac{\lambda}{2}\left[1+\tanh(\frac{\phi_0-\phi}{\sigma})\right]$ (red), where $V_0(\phi) = Ae^{-\sqrt{\frac{2}{q}}\frac{\phi}{M_{Pl}}}$. A. Gallego et al. Eur. Phys. J. **C76**, 385 (2016).

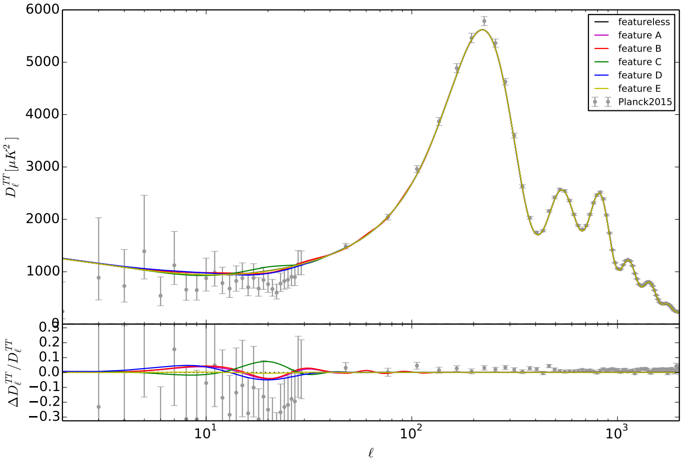

Figure: D_l^{TT} respect to the multipole l, and the relative difference respect to the featureless behavior. A. Gallego et al. Eur. Phys. J. **C76**, 385 (2016).

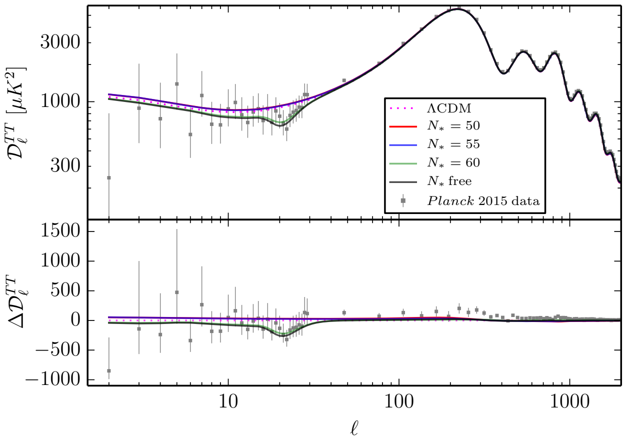

Figure: D_l^{TT} respect to the multipole l, and the relative difference respect to the featureless behavior. Image credit: Yi-Fu Cai et al. Phys. Rev. D 92, (2015).

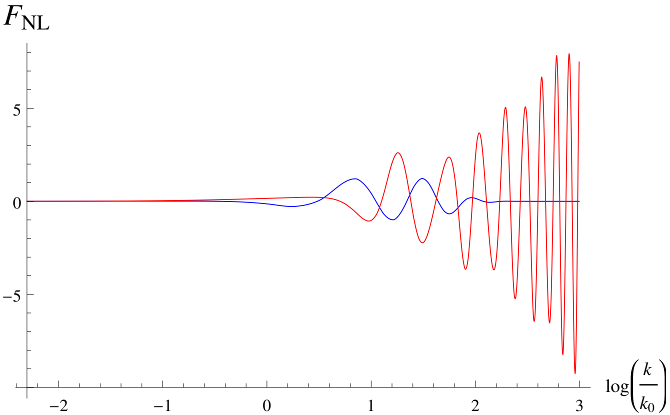

Figure: The equilateral limit of the numerically computed bispectrum F_{NL} for LF (blue) and BF (red). A. Gallego et al. Eur. Phys. J. **C75**, 589 (2015) and Eur. Phys. J. **C76**, 385 (2016).

Conclusions

- Each different type of feature has distinctive effects on the spectrum and bispectrum of curvature perturbations.
- Find mechanisms to produce these potentials.
- Use a more suitable V_0 potential.
- Inflation?

¡GRACIAS!

¡Y FELICITACIONES A LOS PROFESORES LUIS HERRERA Y RODOLFO GAMBINI!

Bibliography

Planck Collaboration, P. Ade *et al.*,
(2015), arXiv:1502.02114, arXiv:1502.01589.

S. Gariazzo, C. Giunti, and M. Laveder,
JCAP **1504**, 023 (2015), arXiv:1412.7405.

A. Gallego Cadavid and A. E. Romano,
Eur. Phys. J. **C75**, 589 (2015), arXiv:1404.2985.

A. Gallego Cadavid and A. E. Romano,
Nucl. Part. Phys. Proc. **267-269**, 254 (2015).

A. Gallego Cadavid, A. E. Romano, and S. Gariazzo,
Eur. Phys. J. **C76**, 385 (2016), arXiv:1508.05687.